

Measuring the dark matter equation of state

Ana Laura Serra^{1,2★} and Mariano Javier L. Domínguez Romero^{3★}

¹*Dipartimento di Fisica Generale ‘Amedeo Avogadro’, Università degli Studi di Torino, Via P. Giuria 1, I-10125 Torino, Italy*

²*Istituto Nazionale di Fisica Nucleare (INFN), Sezione di Torino, Torino, Italy*

³*Instituto de Astronomía Teórica y Experimental (IATE), Consejo de Investigaciones Científicas y Técnicas de la República Argentina (CONICET), Observatorio Astronómico Córdoba, Universidad Nacional de Córdoba, Laprida 854, X5000BGR Córdoba, Argentina*

Accepted 2011 May 20. Received 2011 May 5; in original form 2011 March 9

ABSTRACT

The nature of the dominant component of galaxies and clusters remains unknown. While the astrophysics community supports the cold dark matter (CDM) paradigm as a clue factor in the current cosmological model, no direct CDM detections have been performed. Faber & Visser have suggested a simple method for measuring the dark matter equation of state that combines kinematic and gravitational lensing data to test the widely adopted assumption of pressureless dark matter. Following this formalism, we have measured the dark matter equation of state for the first time using improved techniques. We have found that the value of the equation-of-state parameter is consistent with pressureless dark matter within the errors. Nevertheless, the measured value is lower than expected because, typically, the masses determined with lensing are larger than those obtained through kinematic methods. We have tested our techniques using simulations and we have also analysed possible sources of error that could invalidate or mimic our results. In light of this result, we can now suggest that understanding the nature of requires a complete general relativistic analysis.

Key words: equation of state – gravitation – gravitational lensing: strong – gravitational lensing: weak – galaxies: kinematics and dynamics – dark matter.

1 INTRODUCTION

Strong evidence, from a large number of independent observations, indicates that dark matter is composed of yet-unknown weakly interacting elementary particles. Since these particles are required to have small random velocities at early times, they are called cold dark matter (CDM). Many solutions have been proposed to explain its presence, but its nature remains obscure. Up to the present day, the hypothesis of pressureless dark matter remains experimentally untested since laboratory experiments have not yielded positive results (Bertone 2010).

Faber & Visser (2006) have conceived a novel approach to calculate the density and pressure profiles of the galactic fluid, with no assumptions about their specific form. Such test is based on General Relativity results, the weak-field condition, and the probe particle speeds involved (photons and stars). In order to carry out an explicit measurement of the dark matter equation of state (EoS), we have applied this test to galaxy clusters presenting gravitational lensing effects. The advantage of galaxy clusters over galaxies is their larger dark matter concentrations and their vast spectroscopic data, which allow to calculate reliable kinematic profiles.

2 A RELATIVISTIC EXPERIMENT

A static spherically symmetric gravitational field is represented by a space–time metric of the form (Misner, Thorne & Wheeler 1973) $ds^2 = -c^2 e^{2\tilde{\Phi}(r)} dt^2 + dr^2/[1 - \frac{2m(r)G}{rc^2}] + r^2 d\Omega^2$, where $\tilde{\Phi}(r) = \Phi(r)/c^2$ and Φ is the gravitational potential.

Resorting to the Einstein field equations with a consistent static and spherically symmetric stress-energy tensor, and using the mass-density definition [$\int 4\pi\rho(r)r^2 = m(r)$], the pressure profiles are

$$\begin{aligned} \frac{8\pi G}{c^4} p_r(r) &= -\frac{2}{r^2} \left[\frac{m(r)G}{c^2 r} - r \tilde{\Phi}'(r) \left(1 - \frac{2m(r)G}{c^2 r} \right) \right], \\ \frac{8\pi G}{c^4} p_t(r) &= -\frac{G}{c^2 r^3} \left[\frac{m'(r)r - m(r)}{c^2} \right] [1 + r \tilde{\Phi}'(r)] + \dots \\ &\quad + \left[1 - \frac{2m(r)G}{c^2 r} \right] \left[\frac{\tilde{\Phi}'(r)}{r} + \tilde{\Phi}'(r)^2 + \tilde{\Phi}''(r) \right], \quad (1) \end{aligned}$$

where $p_r(r)$ and $p_t(r)$ refer to the radial and tangential pressure profiles, respectively, which are completely determined by the two functions $\tilde{\Phi}(r)$ and $m(r)$. If these two functions are obtained from observations, both pressure profiles can be inferred. For a perfect fluid, we expect $p = p_r = p_t$.

When analysing data, it is convenient to assume a simplifying hypothesis. Standard Newtonian physics are obtained in the limit of General Relativity through the following conditions: (i) the gravitational field is weak $\frac{2mG}{c^2 r} \ll 1$, $2\Phi \ll c^2$; (ii) the test probe particle

★E-mail: serra@ph.unito.it (ALS); mardom@oac.uncor.edu (MJLDR)

speeds are slow compared to the speed of light; and (iii) the pressure and matter fluxes are small compared to the mass-energy density. While the first and second conditions are accomplished by galaxies in clusters, photons only fulfil the first condition. The third condition is often applied, since it is related to the nature of the dominant component and to the possibility that this is a pressureless fluid. The novel idea introduced by Faber & Visser (2006) is to avoid the assumption of the third condition.

Under condition (i) the tt component of the Ricci tensor is (Misner et al. 1973) $\nabla^2 \Phi \approx -\mathbf{R}_{tt}$, then $\nabla^2 \Phi \approx \frac{4\pi G}{c^2}(c^2 \rho + p_r + 2p_t)$. Consequently, the function $\Phi(r)$ can be interpreted as the Newtonian gravitational potential $\Phi_N(r)$ if and only if the fluid is pressureless. In the kinematic regime, conditions (i) and (ii) are fulfilled. Due to the second condition, the geodesic equation can be reduced to $\frac{d^2 \mathbf{r}}{dt^2} \approx -\nabla \Phi$, where \mathbf{r} is the position vector of the galaxy and $\Phi(r) \neq \Phi_N(r)$. Then, the mass profile obtained from the kinematic analysis is defined by

$$m_K(r) = \frac{r^2}{G} \Phi'_K \approx \frac{4\pi G}{c^2} \int (c^2 \rho + p_r + 2p_t) r^2 dr,$$

which causes $m_K(r)$ to differ from $m(r)$. On the other hand, in the case of gravitational lensing, photons are the test particles and condition (ii) is not satisfied. Hence, the geodesic equation needs to be solved exactly to understand the influence of the gravitational field. By applying Fermat's principle and considering an effective refractive index (see Faber & Visser 2006 for details), the lensing gravitational potential is defined as

$$2\Phi_{\text{lens}}(r) = \Phi(r) + \int \frac{m(r)}{r^2} dr,$$

where $\nabla^2 \Phi_{\text{lens}}(r) = 4\pi \rho_{\text{lens}}(r)$, then $\Phi_{\text{lens}}(r) = \int \frac{m_{\text{lens}}(r)}{r^2} dr$. This implies $m_{\text{lens}}(r) = \frac{1}{2}m_K(r) + \frac{1}{2}m(r)$. This analysis gives a simple expression for the two functions required to calculate the density and pressure profiles:

$$\Phi(r) = \frac{Gm_K}{r^2}; \quad m(r) = 2m_{\text{lens}}(r) - m_K.$$

It is important to note that a gravitational lensing analysis usually assumes a Newtonian gravitational potential, but in this general case, the effective refractive index – a physical observable of gravitational lensing – requires a more comprehensive definition of the gravitational potential.

3 WEIGHING CLUSTERS OF GALAXIES

The Jeans equation offers a direct way to calculate the mass profile via kinematics:

$$m_K(< r) = -\frac{r\sigma_r^2}{G} \left[\frac{d \ln \rho_n}{d \ln r} + \frac{d \ln \sigma_r^2}{d \ln r} + 2\beta \right],$$

where $m_K(< r)$ is the mass enclosed within a sphere of radius r , ρ_n is the 3D galaxy number density, σ_r is the 3D line-of-sight (l.o.s.) velocity dispersion and β is the anisotropy parameter $\beta = 1 - \langle v_\theta^2 + v_\phi^2 \rangle / (2\langle v_r^2 \rangle)$. An alternative approach was introduced by Diaferio & Geller (1997), who suggested the possibility of measuring cluster masses using only redshifts and celestial coordinates of the galaxies. The method they developed, called the caustic technique (CT), allows to calculate the mass profile at radii larger than the virial radius, where the assumption of dynamical equilibrium is not valid. In a redshift-space diagram (l.o.s. velocity v versus projected distances R from the cluster centre), cluster galaxies are distributed on a characteristic trumpet shape, whose boundaries are

called caustics. Since these caustics are related to the l.o.s. component of the escape velocity, they provide a suitable measure of the cluster mass. The CT is a method for determining the caustic amplitude $\mathcal{A}(r)$ and then the cluster mass profile (see Diaferio & Geller 1997 and Diaferio 2009 for details). In order to calculate the kinematic mass profile, we have applied the following procedure to a simulated cluster extracted from the Millennium Simulation Run (Springel et al. 2005), and two real rich clusters of galaxies (Coma and CL0024). The galaxy systems were selected based on four conditions: approximate spherical symmetry, low level of subclustering, gravitational lensing data measurements (only weak-lensing reconstruction in the case of Coma) and an important number of measured redshifts of galaxies in order to accomplish our assumptions. Coma and CL0024 have 1119 and 271 galaxies within the caustics, respectively.

With the purpose of calculating the mass profile via the Jeans equation, we have used the first steps of the CT to remove interlopers, and an adaptive kernel method (described in Diaferio & Geller 1997) to estimate the density distribution of galaxies in the redshift-space diagram. In this way, we are able to obtain a 1D profile for the l.o.s. velocity dispersion σ_R and the 2D number density profile ρ (which are simply the second and first moments of the density distribution at each R , where R is the projected distance from the centre). Using in this novel way the estimated density distribution of galaxies allows us to measure σ_R and ρ at several radii, in order to recover the kinematic mass profile with high precision.

In all cases, we have used a King profile to fit the number density profile ρ and we have followed the procedure described in Díaz et al. (2005) to obtain the 3D number density ρ_n . In order to determine the velocity dispersion σ_r , we have applied the Abel inversion technique, assuming $\beta = 0$. The 2D and 3D profiles are in good agreement with the real profiles of the simulated cluster. This indicates that the assumption of $\beta = 0$ is quite adequate. Despite this good agreement, and in order to quantify the impact of $\beta(r)$ on the dark matter EoS, we have solved the Jeans equation considering three cases: (1) $\beta = 0$ and $\beta(r)$ determined by a linear fit to (2) the data of the selected simulated cluster and (3) the data from the most massive clusters of the Millennium Simulation (Springel et al. 2005), up to $1 h^{-1}$ Mpc. Fig. 1 shows these three mass profiles, together with the caustic mass profile and the true mass profile [Navarro–Frenk–White (NFW) best fit to the simulated data]. The difference between the upper panels reflects the effect of the number of galaxies tracing the kinematics. To mimic a lensing situation, we have projected the mass of the haloes in the field of the simulated cluster and then we have deprojected the 2D density, assuming that all the mass belongs to one single halo. The differences between the true mass profile and the new ‘fake’ mass profile can be appreciated only at large radii and their best NFW fits are almost indistinguishable.

In the calculation of the EoS, we have combined the tangential and radial pressure, so $w = (p_r + 2p_t)/c^2 3\rho$. As shown in Fig. 1, there is a good agreement between the mass profiles of the simulated cluster (except for case 3), implying a null w parameter (Fig. 2). When ~ 200 galaxies are used, the w parameter profiles differ more significantly. This is mainly due to uncertainties of the mass profile and the EoS parameter determinations, which originate from the low number of galaxies of this simulated cluster. The kinematic mass profiles show also some variance due to the presence of inhomogeneities in the radial distributions of galaxies, related to subclustering.

In Fig. 2, it can also be seen that, when using the mass profile determined via the CT, w adopts a high positive value in the inner

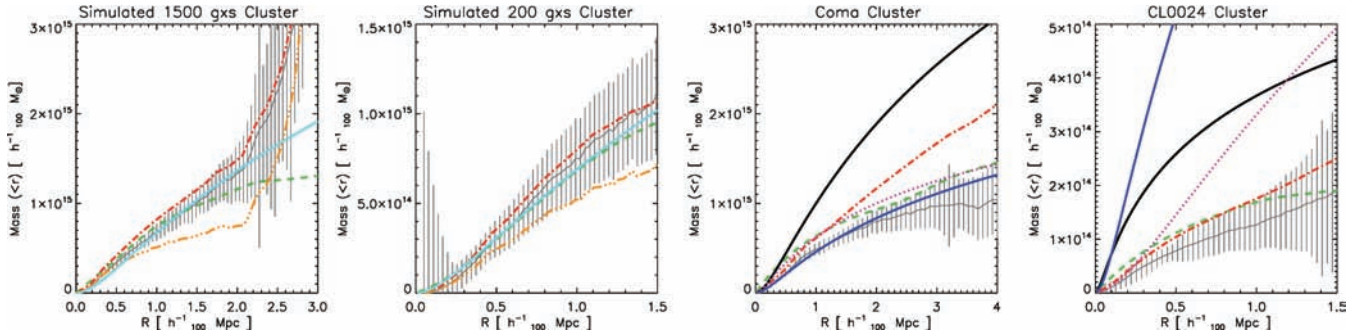


Figure 1. Mass profiles of the simulated (extreme left-hand panel with 1000 galaxies and middle left-hand panel with 200 galaxies) and real clusters (Coma, middle right-hand panel, and CL0024, extreme right-hand panel) for cases 1 (red dot-dashed line), 2 (grey continuous line with error bars from bootstrap analysis) and 3 (orange dash-triple-dotted line, only for simulated clusters) from the CT (green dashed line) and lensing analysis. Lensing profiles are from Kubo et al. (2007) (black continuous line) and Gavazzi et al. (2009) (blue continuous line) in Coma, and from Kneib et al. (2003) (black continuous line) and Umetsu et al. (2010) (blue continuous line) in CL0024. The magenta dotted lines are the NFW kinematic profile from Łokas & Mamon (2003) in Coma and the X-ray-inferred hydrostatic equilibrium mass profile from Ota et al. (2004) in CL0024. In the case of the simulated cluster, the solid cyan line is the NFW fit to the true mass profile, and the kinematic mass profiles were computed by selecting a similar number of galaxies to those for the observed clusters, using a magnitude cut-off.

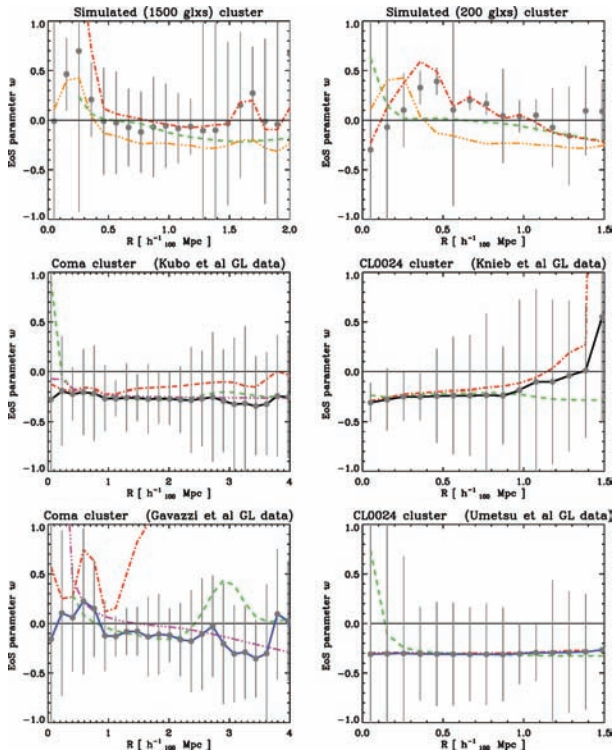


Figure 2. Dark matter EoS radial profiles, corresponding to the mass profiles of Fig. 1, with the same conventions. For clarity, we split the EoS parameter determination based on the different mass density profiles obtained from lensing analysis. Error bars (at the 1σ level) were computed using bootstrap analysis in the galaxy samples used in the determination of the kinematic profile and in the NFW parameters of the dark matter profile inferred from lensing.

regions of the clusters. This might happen because the CT is very effective in estimating the mass profile in the outskirts, but it tends to overestimate it within the virial radius (Serra et al. 2010).

4 MEASUREMENT OF THE DARK MATTER EoS IN COMA AND CL0024

The results of the methods described above show a good agreement between the measured profile and the real mass profile in the case of

the simulated cluster, independently of the number of galaxies used in the computation of the kinematic mass. Our method is slightly sensitive to the anisotropy parameter; to address this problem, we have calculated the EoS with the kinematic mass drawn from cases 1, 2 and 3 (explained in Section 3). The resulting profiles, in Fig. 2, show that the anisotropy parameter β has a non-negligible impact on the EoS. As the first result of this work, we have found, in the case of the real clusters of galaxies, a good agreement between the kinematic mass profiles computed using the CT (heuristic recipe) and the Jeans equation inversion (rigorously correct), but there is a notable difference between them and the mass derived from the gravitational-lens model (Fig. 1, see also Diaferio 2009). However, this discrepancy allows us to measure the dark matter EoS for the first time using clusters of galaxies. The resulting EoS of the dark matter (shown in Fig. 2) behaves as expected when we analyse the simulated cluster, but it adopts an almost constant negative value for the real clusters (however, consistent with the strong energy condition) instead of the constant zero value required by CDM. We could attribute that to the anisotropy parameter β . Nevertheless, the CT is not strongly dependent on β , and the EoS from the caustic profile also shows a trend to be negative. We have checked a number of sources of systematics such as the departure of sphericity and relaxation, the presence of deflecting substructures in the l.o.s. (as those reported in Coma by Adami et al. 2009) and the ellipticity of the halo. We have tested the lack of sphericity by computing the mass profiles along three different l.o.s., showing no significant differences. The presence of substructures in the l.o.s. has been evaluated not only through the redshift distribution of the cluster galaxies, but also through deprojecting the 2D mass, assuming that the mass of the haloes near the l.o.s. belongs to the same cluster (as explained in Section 3). As for the triaxiality of the halo, we have modified the NFW parameters of the lensing mass, according to the results presented in Corless & King (2007), considering an extreme case of the axial ratio $Q = 2.5$. None of these tests seems to explain the features we have shown (Serra 2008), although we stress that a combination of several of them might be responsible for this apparent inconsistency.

It should be mentioned that the cluster of galaxies CL0024 experienced a merger along the l.o.s. (Czoske et al. 2002) approximately 2–3 Gyr ago. Nevertheless, the good agreement between the kinematic mass profile computed and the Ota et al. (2004) hydrostatical equilibrium mass in the inner region indicates that the gravitational

potential has had time to relax (this was noted first by Umetsu et al. 2010). The density profiles determined by lensing methods in CL0024 (Kneib et al. 2003; Umetsu et al. 2010) are in good agreement with each other. This is not the case for Coma, but it should be recalled that the Coma density profile derived from the weak-lensing analysis of Gavazzi et al. (2009) was computed in the central region ($R < 1$ Mpc) using a very deep photometry. This density profile was extrapolated to outer radii in our analysis, and the w parameter computed using this profile shows a fair agreement with the CDM value. The weak-lensing profile of Kubo et al. (2007) spans a much wider region using SDSS photometry, and the corresponding w has a constant and negative value.

The EoS parameter recovered using this lensing analysis in Coma shows a similar behaviour to those obtained in CL0024 (i.e. a preferred value of $w \sim -\frac{1}{3}$). There is, however, a trend for the w computed with the lensing profile from Kneib et al. (2003) to increase towards the external regions. If further measurements confirm the trend of negative values for the dark matter EoS w , then this result could be interpreted in the framework of theories including scalar fields and the possibility of effective negative pressures, or alternative models of gravity. It is important to note that the measured value of w in this work is consistent with the standard pressureless CDM at the 1σ level. The error analysis uses 30 bootstrap samples of the galaxies in the computation of the kinematic mass profiles, and 30 dark matter profiles resulting from the errors and degeneracies of the measurements of the NFW halo parameters. The assumption of pressureless dark matter can be further tested by applying the method introduced in this work to a large number of lensing clusters with several galaxy members with measured redshifts.

ACKNOWLEDGMENTS

We acknowledge the constructive comments from the anonymous referee. We thank Dr Diego García Lambas, Dr Héctor Vucetich, Dr Osvaldo Moreschi and Dr Antonaldo Diaferio for many helpful suggestions and comments. The Millennium Run simulation used in this Letter was carried out by the Virgo Supercomputing Consor-

tium at the Computing Centre of the Max-Planck Society in Garching. The semi-analytic galaxy catalogue is publicly available at <http://www.mpa-garching.mpg.de/galform/agnpaper>. This research has made use of the SIMBAD data base, operated at CDS, Strasbourg, France. This work has been partially supported by Consejo de Investigaciones Científicas y Técnicas de la República Argentina (CONICET). Support from the INFN grant PD51 and the PRIN-MIUR-2008 grant ‘2008NR3EBK 003’ ‘Matter-antimatter asymmetry, dark matter and dark energy in the LHC era’ is gratefully acknowledged. MJLDR also warmly thanks Dr J. Bass, Dr A. Valle and Dr N. Gándara for their long commitment to public service.

REFERENCES

- Adami C. et al., 2009, *A&A*, 507, 1225
- Bertone G., 2010, *Nat*, 468, 389
- Corless V. L., King L. J., 2007, *MNRAS*, 380, 149
- Czoske O., Moore B., Kneib J.-P., Soucail G., 2002, *A&A*, 386, 31
- Diaferio A., 2009, preprint (arXiv:0901.0868)
- Diaferio A., Geller M. J., 1997, *ApJ*, 481, 633
- Díaz E., Zandivarez A., Merchán M. E., Muriel H., 2005, *ApJ*, 629, 158
- Faber T., Visser M., 2006, *MNRAS*, 372, 136
- Gavazzi R., Adami C., Durret F., Cuillandre J., Ilbert O., Mazure A., Pelló R., Ulmer M. P., 2009, *A&A*, 498, L33
- Kneib J.-P. et al., 2003, *ApJ*, 598, 804
- Kubo J. M., Stebbins A., Annis J., Dell’Antonio I. P., Lin H., Khiabani H., Frieman J. A., 2007, *ApJ*, 671, 1466
- Łokas E. L., Mamon G. A., 2003, *MNRAS*, 343, 401
- Misner C. W., Thorne K. S., Wheeler J. A., 1973, *Gravitation*. W. H. Freeman and Co., San Francisco
- Ota N., Pointecouteau E., Hattori M., Mitsuda K., 2004, *ApJ*, 601, 120
- Serra A. L., 2008, *FaMAF*, Universidad Nacional de Córdoba, Argentina, Trabajo final de Licenciatura en Astronomía
- Serra A. L., Diaferio A., Murante G., Borgani S., 2010, *MNRAS*, 412, 800
- Springel V. et al., 2005, *Nat*, 435, 629
- Umetsu K., Medezinski E., Broadhurst T., Zitrin A., Okabe N., Hsieh B., Molnar S. M., 2010, *ApJ*, 714, 1470

This paper has been typeset from a \LaTeX file prepared by the author.